



1 EERA DeepWind'2014, 11th Deep Sea Offshore Wind R&D Conference

2 **Characterization of the SUMO turbulence measurement system for**  
3 **wind turbine wake assessment**

4 Line Båserud\*, Martin Flügge, Anak Bhandari, Joachim Reuder

5 *Geophysical Institute, University of Bergen, Allegaten 70, N-5007 Bergen, Norway*

6 **Abstract**

7 The remotely piloted aircraft system (RPAS) SUMO (Small Unmanned Meteorological Observer) has been equipped with a  
8 miniaturized 5-hole probe sensor system for measurement of the 3-dimensional flow vector with a temporal resolution of 100 Hz.  
9 Due to its' weight and size this system is particularly well suited for operations in the vicinity of wind turbines. To qualify for full  
10 scale measurements in turbine wakes the system has been characterized by several laboratory and field tests described in this study.

11 A wind tunnel test against a hot-wire anemometer shows the capability of the 5-hole probe to react to turbulence in the same  
12 manner as the hot-wire system. The resulting spectra from the two platforms show in general good agreement for both laminar and  
13 turbulent flows. The 5-hole probe system is able to resolve turbulence up to frequencies around 20 – 30 Hz when using a tubing  
14 length of 15 cm between the probe and the pressure transducers.

15 In addition, an environmental parallel test against two sonic anemometers mounted on the roof-top of a car was performed at  
16 Bergen airport Flesland. Despite several issues with the self-made and low-cost experimental setup, important system character-  
17 istics could be tested and verified. In particular the velocity spectral components of the sonic anemometer system and the 5-hole  
18 probe are in close resemblance to each other. This is at least a strong indication that the 5-hole probe is suitable for atmospheric  
19 turbulence measurements onboard the RPAS SUMO platform.

20 © 2014 Published by Elsevier Ltd. This is an open access article under the CC BY-NC-ND license  
(<http://creativecommons.org/licenses/by-nc-nd/3.0/>).

Selection and peer-review under responsibility of SINTEF Energi AS

21 *Keywords:* atmospheric boundary layer (ABL); turbulence; remotely piloted aircraft system (RPAS); wind turbine wake; wind energy;  
22

23 **1. Introduction**

24 The interaction between wind turbines and the atmospheric boundary layer is highly complex. The resulting wind  
25 turbine wakes are characterized by high temporal and spatial variability. Their extension and dynamics strongly de-  
26 pend on atmospheric stability, which is the crucial factor controlling the interplay between the relevant flow conditions  
27 given by the profiles of wind speed, i.e. wind shear, and turbulence intensity. A turbine wake is mainly characterized  
28 by a reduction of the average wind speed and the increase of the turbulence level that negatively effects the productivity  
29 and fatigue load of downstream turbines in a wind farm. The proper understanding of the development and structure

\* Corresponding author. Tel.: +47-55588433 ; fax: +47-55589883.  
E-mail address: [line.baserud@gf.uib.no](mailto:line.baserud@gf.uib.no)

30 of a single turbine wake is therefore of uttermost importance. The detailed investigation of the dynamical behavior of  
31 such wakes, e.g. meandering or the dispersion of the wake zone with the downstream distance, requires both modeling  
32 and full scale observations. During the last years, corresponding CFD simulations have been performed with varying  
33 but in general increasing complexity (e.g. [1]). Required full scale data sets for the improved understanding of the  
34 underlying physical processes and the initialization, test and validation of such simulations are sparse at the best. One  
35 of the main reasons is the instrumental and infrastructural demand connected to corresponding observations. With the  
36 development and application of ground based scanning lidar systems and nacelle based static units looking backwards  
37 in the turbine wake, the observational basis is however expected to improve in the future (e.g. [2], [3]).

38 Most of the existing knowledge is based on records from in-situ measurements at meteorological masts and towers  
39 or on ground based remote sensing (e.g.[4]) by lidar [5–7], sodar [8] [9] and lately also radar [10]. Static masts and  
40 towers mainly lack positioning flexibility with respect to the high temporal and spatial variability of the wake and  
41 are in addition rather expensive, at least when completely covering the relevant altitude level of state-of-the-art wind  
42 turbines extending 150 m. Moreover, the interpretation of spatial structures based on point measurements requires the  
43 validity of Taylor’s hypothesis of frozen turbulence [11] [12] which cannot be guaranteed in such a highly turbulent  
44 environment. The remote sensing sensors can only provide volume averages of the wind speed distribution and the  
45 spatial resolution of the systems nowadays in use, typically in the order of several tens of meters, is not sufficient for  
46 a detailed structural investigation of the wake.

47 In-situ airborne measurements can provide novel and highly relevant data sets in this field. Manned aircraft opera-  
48 tions in a wind farm or in the vicinity of a single wind turbine are out of question due to safety considerations. Small  
49 and light-weight Remotely Piloted Aircraft Systems (RPAS) however can operate safely in such an environment [13]  
50 [14]. The miniaturization of electronics and sensors in the last years has now allowed to equip even very light RPAS  
51 with a take-off weight clearly below 1 kg with sensors for the measurement of the turbulent flow vector [15] [16]. Sys-  
52 tems of this size and weight will not jeopardize the tower or the turbine blades even in the unlikely event of a collision  
53 of the RPAS with the structure. However, appropriate strategies for the used flight patterns and the after-flight data  
54 processing and interpretation have to be developed, keeping in mind that a single RPAS will only be able to provide a  
55 snapshot of the actual situation. The potential of simultaneous operation of several RPAS in the future would also be  
56 of invaluable benefit in this context.

57 The determination of reliable turbulence data sets from airborne platforms requires on one hand a careful char-  
58 acterization of the spectral response of the system to ensure that structures in the relevant scale can be resolved  
59 appropriately. On the other hand, adequate motion correction algorithms have to be applied to correct for the aircraft’s  
60 attitude and motion during the turbulence measurements [17–20].

61 This paper is structured as follows. Section 2 shortly presents the recent, improved version of the SUMO system  
62 for turbulence measurement based on a 5-hole flow probe. The results of laboratory wind tunnel tests of the spectral  
63 response in comparison with a hot-wire anemometer are described in section 3. The potential effect of the tubing  
64 length between the probe and the pressure transducers has also been addressed in this part. Section 4 shows the results  
65 of an environmental test of the system by parallel measurements with a sonic anemometer mounted on a car. Finally  
66 a short summary and outlook is given in section 5.

## 67 2. The SUMO turbulence measurement system

68 The atmospheric turbulence measurement system developed for the future in-situ investigation of single turbine  
69 wakes presented here consists of the micro RPAS SUMO [15] [16] as sensor carrier and a commercially available  
70 5-hole probe system for the measurement of the 3-dimensional turbulent wind vector. The fixed-wing model aircraft  
71 FunJet from Multiplex works as the basis for the SUMO airframe. The system has been developed and continuously  
72 improved over the last 7 years in close cooperation between the Geophysical Institute, University of Bergen, Norway  
73 and Lindenberg und Müller GmbH & Co. KG, Germany. SUMO is driven by a single propeller in the rear, electrically  
74 powered by a LiPo battery pack, enabling flight times of up to 40 min. With its take-off weight of around 600 g, a  
75 wingspan of 0.80 m and a length 0.75 m, SUMO provides a small and flexible measurement platform. It operates at  
76 cruise speeds of 12 - 25 m s<sup>-1</sup>. For navigation and automatic flight, SUMO uses the open source autopilot system  
77 Paparazzi [21] developed and maintained by the École National de l’Aviation Civile (ENAC) in Toulouse, France.

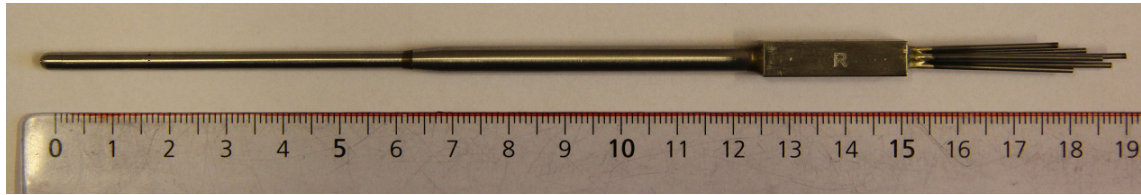


Fig. 1: The 5-hole probe from Aeroprope Cooperations.

78 Continuously updated software and detailed description of hardware are freely available from the project website.  
79 Predefined flight plans can be flown autonomously and changes can be made at any time during a flight mission.

80 The SUMO airframe is operationally equipped with meteorological sensors for measurement of temperature and  
81 relative humidity (Sensirion SHT 75), pressure (M55611), and an downward directed IR sensor (MLX90247) for the  
82 estimation of the surface temperature. For the measurement of the 3-dimensional turbulent flow vector with a temporal  
83 resolution of 100 Hz the SUMO system can be extended by the Air Data System (ADS) from Aeroprope Corporation.  
84 It consists of an air data computer and a miniaturized 5-hole probe with corresponding pressure transducers [22]. A  
85 soft plastic tubing (TYGON R-3603 [23]) connects the probe to the air data computer, which is placed inside the front  
86 compartment of the SUMO fuselage. The 5-hole probe itself is placed at the nose of the aircraft, with the sensing area  
87 about 10 cm in front of the nose tip, to minimize the effects of flow distortion induced by the airframe.

88 Fig. 1 shows the 5-hole probe. It is constructed in stainless steel and has a length of 15 cm and a diameter of 3 mm.  
89 The probe measures static and dynamic pressures through small holes at its side and tip. The resulting ADS output  
90 parameters, based on these differential pressure measurements, are the true airspeed (TAS), angle of attack ( $\alpha$ ), angle  
91 of sideslip ( $\beta$ ) and altitude. The output can either be stored on a Micro-SD card on board or streamed directly to a  
92 PC through a serial RS-232 connection. The first option is used for SUMO flight missions while the latter is ideal for  
93 online monitoring, e.g. during system tests and laboratory calibrations.

94 The latest version of SUMO can store both the 5-hole probe turbulence measurements and the attitude information,  
95 i.e. the aircraft's pitch, roll and yaw as well as the linear and angular accelerations from the autopilot's inertial  
96 measurement unit (IMU), on one common data logger. This avoids previously needed work and challenges in connection  
97 with motion correction based on two unsynchronized data sets [16] [13]. The sampling frequency of the aircraft  
98 attitude is now in addition increased from 10 Hz to 60 Hz.

### 99 3. Wind tunnel tests of the 5-hole probe system

#### 100 3.1. Measurement setup

101 A laboratory experiment took place in April 2013 in a wind tunnel at the University of Applied Sciences Regens-  
102 burg, Germany, in order to validate the performance of the 5-hole probe ADS. The system was first tested in a parallel  
103 experiment together with a hot-wire anemometer (HW) for a comparison of the spectral response of the two systems.  
104 Thereafter the effect of varying tubing length between the probe and the air data computer was tested to investigate  
105 potential effects of spectral damping induced by the tubing. All tests were first conducted in laminar and then turbu-  
106 lent conditions, both with a background flow of  $18 \text{ m s}^{-1}$ . This flow speed was chosen since SUMO usually operates  
107 in the range of 12 to  $25 \text{ m s}^{-1}$  during scientific flight missions. The turbulence was created by a horizontal stick in  
108 the flow ( $\sim 3 \text{ cm}$  diameter) upstream of the sensors. The simple mechanism used to create turbulence in these tests  
109 cannot be expected to fully reproduce atmospheric turbulence. However, the intention of the experiments was a gen-  
110 eral characterization of the spectral response of the 5-hole probe ADS compared to a well established measurement  
111 platform.

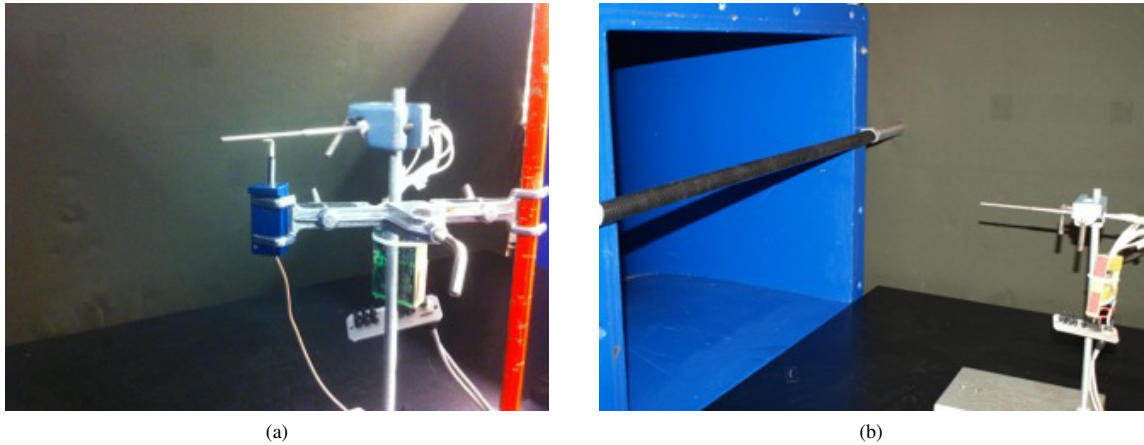


Fig. 2: The mounting of the 5-hole probe in the wind tunnel (a) and the experimental setup for the turbulent flow, with a horizontal stick upstream of the probe (b). Pictures by Sebastian Wein.

112 The HW system (model StreamLine from Dantec) and the 5-hole probe ADS have been deployed alongside in  
 113 the wind tunnel and placed straight in the flow direction, i.e. the probe angle of attack and angle of sideslip had no  
 114 offset from the horizontal plane and the centerline respectively. All experiments had a duration of 5 min. With an  
 115 original temporal resolution of 5 kHz, the HW measurements have been averaged to 100 Hz which corresponds to  
 116 the sampling frequency of the 5-hole probe ADS. The ADS used the original tubing length of 15 cm for all parallel  
 117 experiments. The HW system measured the airspeed and the ADS measured airspeed (TAS), angle of attack ( $\alpha$ ) and  
 118 angle of sideslip ( $\beta$ ).

119 The soft plastic tubing between the probe and the air data computer is responsible for transferring the incoming  
 120 pressure signal to the pressure transducers. In a second test, the system was deployed alone in the wind tunnel and  
 121 tested for the three tubing lengths of 15 cm (short tubing), 30 cm (medium tubing) and 90 cm (long tubing). The short  
 122 tubing of 15 cm resembles the length already being used by SUMO for the first field campaigns. A longer tubing  
 123 would be required if the positioning of the probe has to be changed, e.g. in case future wind tunnel tests reveal a  
 124 considerable effect of flow distortion for the recent mounting at the aircraft nose.

### 125 3.2. Results of wind tunnel tests

126 Fig. 3 shows the averaged spectra of the airspeed component from the hot-wire anemometer (HW) and the 5-  
 127 hole probe ADS under laminar (left) and turbulent (right) conditions. A marked difference in spectral energy density  
 128 ( $S(f)$ ) is visible between the laminar and turbulent case for both measurement systems. In the higher frequency range  
 129 the non-turbulent spectra have an energy level of about  $10^{-4} \text{ m}^2 \text{ s}^{-2}$  while the turbulent spectra reach values around  
 130  $10^{-1} \text{ m}^2 \text{ s}^{-2}$ , namely three orders of magnitude higher.

131 The spectra from the two platforms show in general good agreement in the relevant frequency range ( $> 0.02 \text{ Hz}$ ).  
 132 The 5-hole probe ADS reacts to the turbulence in the same manner as the HW system. The small difference between  
 133 the ADS and HW spectra in both cases is nearly constant, suggesting a similar response to the turbulence, but with a  
 134 difference in variability. The slightly higher energy level of the 5-hole probe ADS compared to the HW for laminar test  
 135 conditions could indicate an enhanced basic noise level of the ADS compared to the HW. Under turbulent conditions,  
 136 it is the HW system that has the highest energy level. Here the higher variability in the HW measurements can be  
 137 explained by the higher temporal resolution of the system, when picking out instantaneous samples from 5 kHz data  
 138 every 0.01 s to have directly comparable measurements to the 100 Hz ADS.

139 Fig. 4 presents the spectra of TAS,  $\alpha$  and  $\beta$  for three different tubing lengths under laminar (left panels) and  
 140 turbulent (right panels) conditions. The tubing lengths are indicated by the colors red (short), black (medium) and  
 141 green (long). All parameters experience again the energy shift of 3 orders of magnitude between laminar and turbulent  
 142 conditions. Variation of the tubing length has little effect under laminar conditions. All spectra lie approximately at  
 143 the same energy level and keep this level throughout the high frequency range. Under turbulent conditions, the spectra  
 144 vary more for the different tubing lengths. For the shortest tubing length of 15 cm, already being used when operating  
 145 the ADS in SUMO, the TAS,  $\alpha$  and  $\beta$  all experience a weak energy loss above 20 – 30 Hz. The use of medium or  
 146 long tubing results in a bigger energy loss, which also starts at lower frequencies (around 10 Hz). The increase in  
 147 spectral damping for the longer tubing lengths suggests that the shortest one is the best of the three options. A wave-  
 148 or resonance effect can probably explain the observed energy loss. The ADS manual states that the tubing should be  
 149 kept as short as possible in order to not limit the response between the probe and the air data computer [22], and our  
 150 experiments seem to agree.

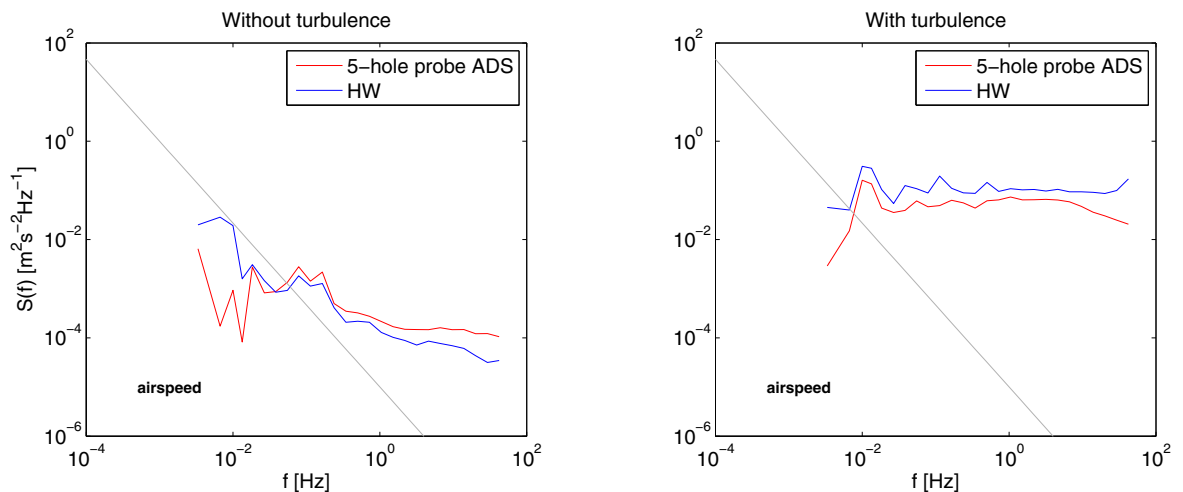


Fig. 3: Averaged power spectra of airspeed measured by the ADS (red) and the HW (blue) systems for the parallel setup, with frequency ( $f$ ) on the x-axis and spectral energy density ( $S(f)$ ) on the y-axis. The laminar case to the left and the turbulent case to the right. The grey line represents the  $-5/3$  slope expected for the inertial subrange of a Kolmogorov spectrum.

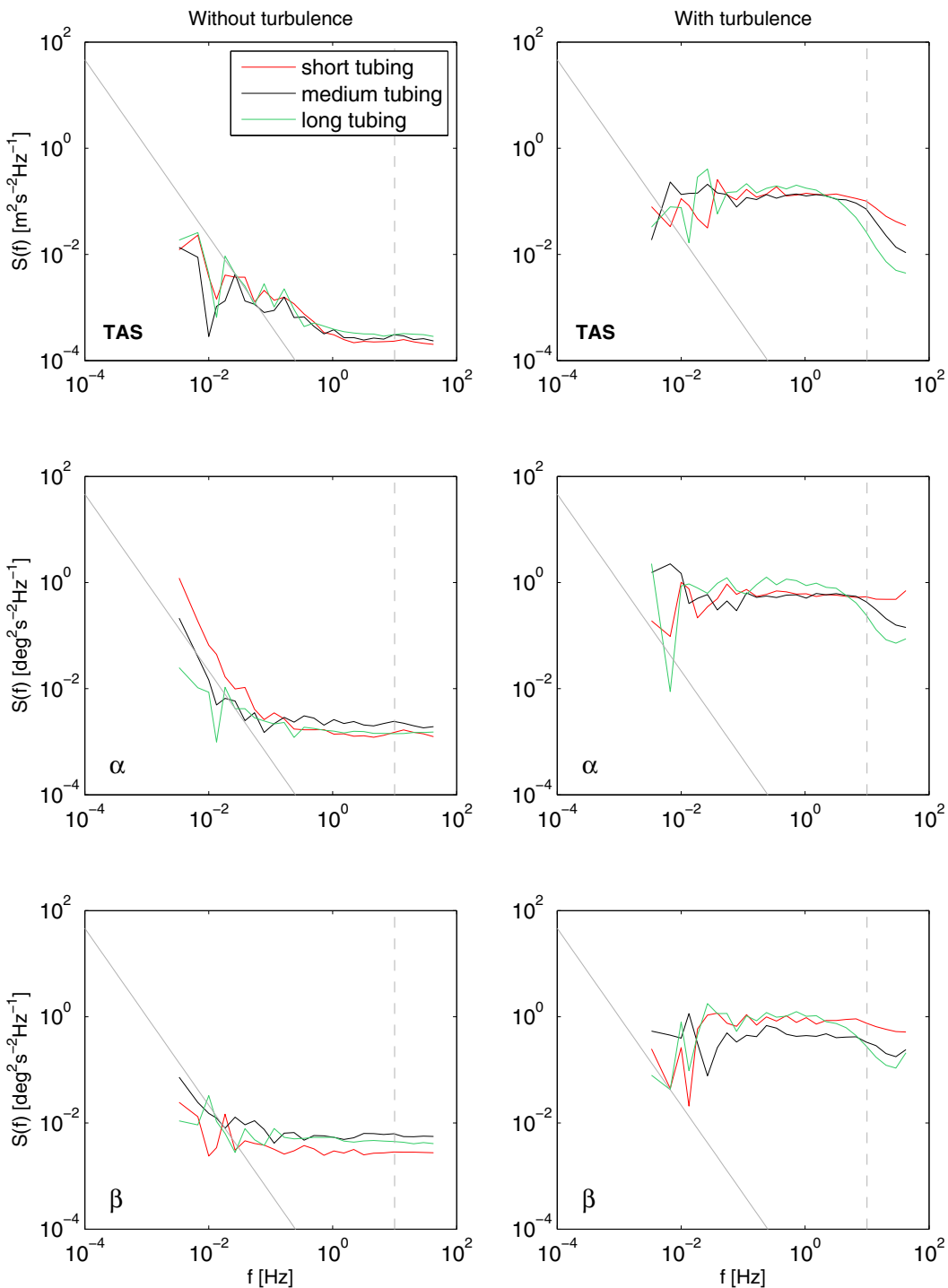


Fig. 4: Averaged power spectra of airspeed (top panel), angle of attack (middle panel) and angle of sideslip (bottom panel) from the 5-hole probe ADS. Again with the frequency ( $f$ ) on the x-axis and spectral energy density ( $S(f)$ ) on the y-axis. Tubing length is indicated by the colors, red (short tubing - 15 cm), black (medium tubing - 30 cm) and green (long tubing - 90 cm). The laminar case is shown to the left and the turbulent case to the right. The frequency of 10 Hz is indicated by the dashed grey line, while the solid grey line represents the  $-5/3$  slope expected for the inertial subrange of a Kolmogorov spectrum.



#### 151 4. Environmental test of the 5-hole probe system

##### 152 4.1. Measurement setup

153 As a next step after the laboratory experiments at only very low turbulence levels, the 5-hole probe system was  
154 tested under real atmospheric turbulence conditions. The 5-hole probe ADS mounted on a SUMO dummy airframe  
155 was deployed together with two different sonic anemometer systems, one Campbell CSAT 3 and one Gill R3-100,  
156 on the roof-top of the institute car, a Ford Transit model 1995. The R3-100, hereafter referred to as the DCF (Direct  
157 Covariance Flux) system, is originally part of an offshore based turbulence measurement system and therefore also  
158 equipped with an inertial measurement unit (IMU) for motion correction purposes [24]. The test was performed in  
159 the early morning of October 25, 2013, on the runway of Bergen airport Flesland.

160 Fig. 5 shows the instrument placement on an extension arm slightly in front of the vehicle. Two ladders secured  
161 to the roof racks of the car served as the basis for the extension arm. A customized frame in aluminium and wood  
162 was mounted on top as sensor platform. All three measurement systems were placed at the same height level, with  
163 a horizontal separation of 48 cm. The SUMO dummy with the 5-hole probe ADS on board was mounted in the  
164 center, with the CSAT3 to its right and the DCF system to the left. The tip of the 5-hole probe was aligned with the  
165 center of the measurement volumes of both sonic anemometers. The mobile laboratory of Gordon et al. [25], used for  
166 turbulence measurements behind trucks on highways in Canada, provided the inspiration for the selected experimental  
167 setup.

168 The car was operated for 12 straight legs each of ca. 3 km length. Consecutive legs were run in opposite directions  
169 down the runway (runway heading 17/35) using the constant car speeds of 20 and 25 m s<sup>-1</sup>. The test was performed in  
170 a window of no precipitation, with weak winds of about 1-2 m s<sup>-1</sup>, and a temperature of around 7.5 °C. Unfortunately,  
171 the CSAT3 did not work properly and only data from the DCF system will be compared to the SUMO measurements.

172

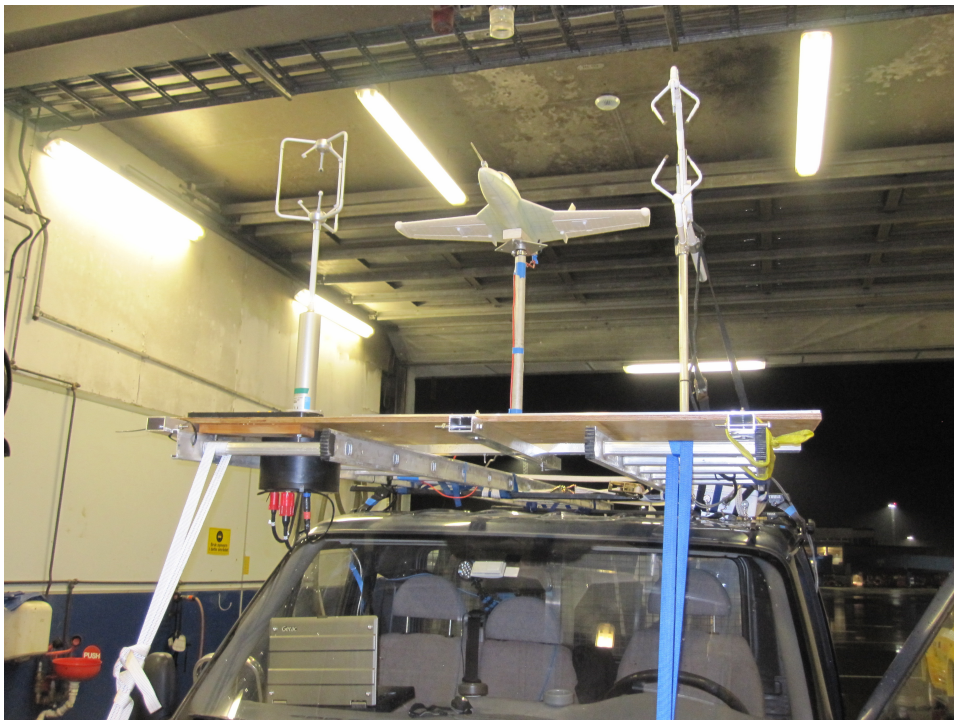


Fig. 5: The experimental setup for the test campaign at Flesland airport in Bergen. From left to right: Gill R3-100 sonic anemometer, SUMO dummy with the 5-hole turbulence probe, Campbell CSAT3 sonic anemometer

173 Uncorrected measurements of the longitudinal (U), lateral (V) and vertical (W) velocity components are shown in  
 174 Fig. 6. A motion correction is necessary as the measurements have been performed from a moving platform. While  
 175 the vibrations caused by the diesel engine of the car should be negligible, the mounting frame of the instrumentation  
 176 on the roof-top might have been exposed to surge and sway motions when driving over uneven parts of the runway.  
 177 In addition, we expected the mounting frame to be slightly lifted as a function of the incoming airflow when driving  
 178 the car. The anemometer and the 5-hole probe also have to be corrected for instrumentation tilt offsets (e.g. [26]) so  
 179 that all measurements can be compared in the same reference plane.

180 For simplicity, we chose to rotate the local coordinate systems of the SUMO and the DCF into the car's right-  
 181 handed frame of reference which is defined as: x-axis pointing forward, y-axis pointing to the left and z-axis pointing  
 182 upward. The tilt angles (e.g. pitch and roll) of the instruments coordinate systems are given from the respective  
 183 IMU's and can be directly used in the transformation matrix  $\mathbf{T}$  ([27]) which rotates the wind speeds recorded in the  
 184 instrument coordinate systems into the car coordinate system. The IMU's accelerometers and angular rate sensors also  
 185 recorded surge and sway motions of the DCF and the SUMO dummy. These oscillating motions induce an additional  
 186 velocity component ( $\mathbf{U}_{plat}$ ) which has to be added to the rotated wind measurements of the 5-hole probe ADS and the  
 187 sonic anemometer respectively. This velocity component is assessed by rotation of the accelerometer outputs into the  
 188 car's reference frame, followed by subsequent integration and high-pass filtering. The recorded longitudinal velocity  
 189 component of both systems is finally corrected by subtraction of the car's velocity. The complete motion correction  
 190 procedure can be found elsewhere in the literature (e.g. [18,28,29]).

191 Application of the motion correction procedure showed that the surge and sway motions of the both instrument  
 192 platforms are small ( $\mathcal{O}(\mathbf{U}_{plat}) = 10^2$ ) compared to the recorded wind speeds, which was to be expected as the car was  
 193 operated on a straight airport runway. This simplifies the correction procedure to

$$194 \quad \mathbf{U}_{true}^{car} = \mathbf{T}(\mathbf{U}_{rec}) - Lp[\mathbf{V}_{GPS}] \quad (1)$$

195 where  $\mathbf{U}_{true}^{car}$  is the corrected wind vector in the car reference frame,  $\mathbf{T}$  denotes the transformation matrix for coordi-  
 196 nate system rotation,  $\mathbf{U}_{rec}$  the recorded wind velocity vector in the instrument frame,  $\mathbf{V}_{GPS}$  is the car's velocity vector  
 197 over ground given by the instrument platform's GPS systems and  $Lp$  denotes a low-pass filter operator.

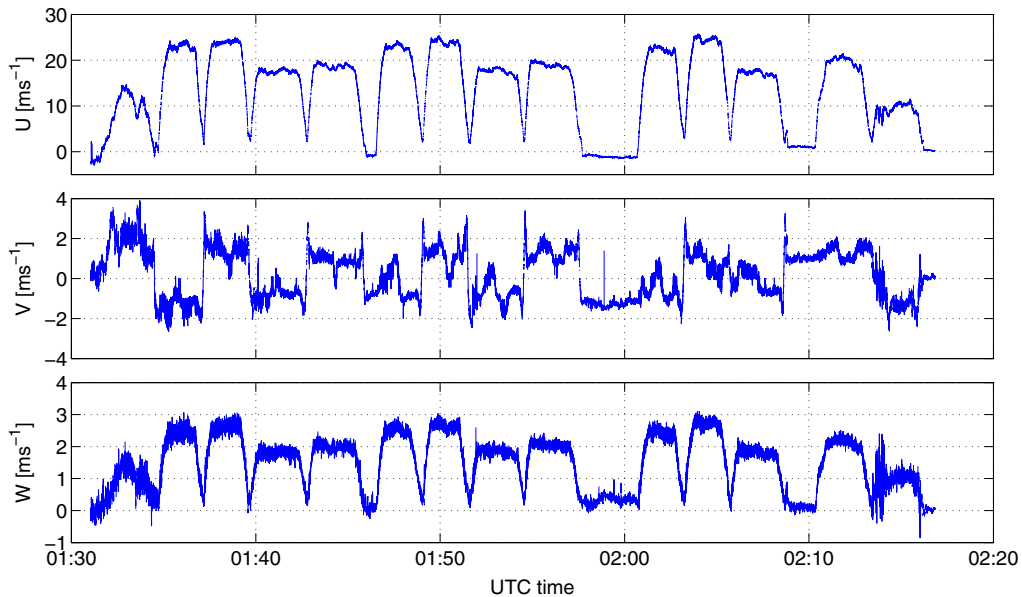


Fig. 6: Time-series of the longitudinal (U - in direction of the moving car), lateral (V - crosswind) and vertical (W) components of the measured flow vector from the DCF system.



## 198 4.2. Results of environmental test

199 To investigate the behavior of the 5-hole probe ADS under real atmospheric conditions, the spectral response of  
 200  $U$ ,  $V$  and  $W$  components from SUMO are compared to those obtained from the Gill sonic anemometer (DCF system)  
 201 when driving with both instruments on the roof-top of the institute car (Fig. 7).

202 The 100 Hz TAS data of the 5-hole probe ADS and the 60 Hz attitude information of the SUMO aircraft have  
 203 been re-sampled to 50 Hz to match the frequency of the DCF system. Vibrations of the instrument mounting result in  
 204 several spectral peaks which are removed by the motion correction procedure. Unfortunately, the accelerometers of  
 205 the SUMO system were only running with a low frequency resolution due to technical limitations at the time of the  
 206 field test. As a consequence, the frequency peaks, which are clearly seen in the 5-hole probe ADS spectra between 1  
 207 and 10 Hz, could not be removed at this instance. Nevertheless, we emphasize that the measured velocity components  
 208 introduced by the mounting vibrations are small compared to the measured wind speeds.

209 Both panels of Fig. 7 show enhanced spectral energy ( $fS(f)$ ) for all velocity components at the low- and high-  
 210 frequency end. Higher spectral energy at the low-frequency end ( $f < 10^{-1}$ ) of the horizontal spectra is likely due to  
 211 the low-frequency oscillations of the car speed which was varying around the target velocity of 20 and 25  $\text{m s}^{-1}$  (see  
 212 upper panel of Fig. 6). The enhanced spectral energy at the low-frequency end of the vertical velocity spectra is likely  
 213 due to the low-frequency oscillations of the mounting frame. Analysis of both systems pitch angles revealed that the  
 214 frame was slightly lifted upward by the incoming air-flow as a function of the car speed.

215 The increased spectral energy at the high-frequency end of the DCF-spectra is likely to be a result of flow distortion  
 216 from the straps used to fix the ladders (see Fig. 5). The horizontal velocity spectra of the 5-hole probe ADS roughly  
 217 follow the theoretically expected  $-2/3$  slope of the inertial subrange for both velocity intervals. However, the vertical  
 218 spectra of the 5-hole probe ADS is not following the expected slope for the car speed of 20  $\text{m s}^{-1}$ , indicating to be  
 219 affected by flow distortion. This might be a consequence of the increase of vertical velocity with car speed (see lower  
 220 panel of Fig. 6). Together with the slight variations in the pitch angle during the experiment lead us to conclude that  
 221 the mounting frame decelerate and deflect the horizontal airflow in front of the car, introducing an vertical velocity

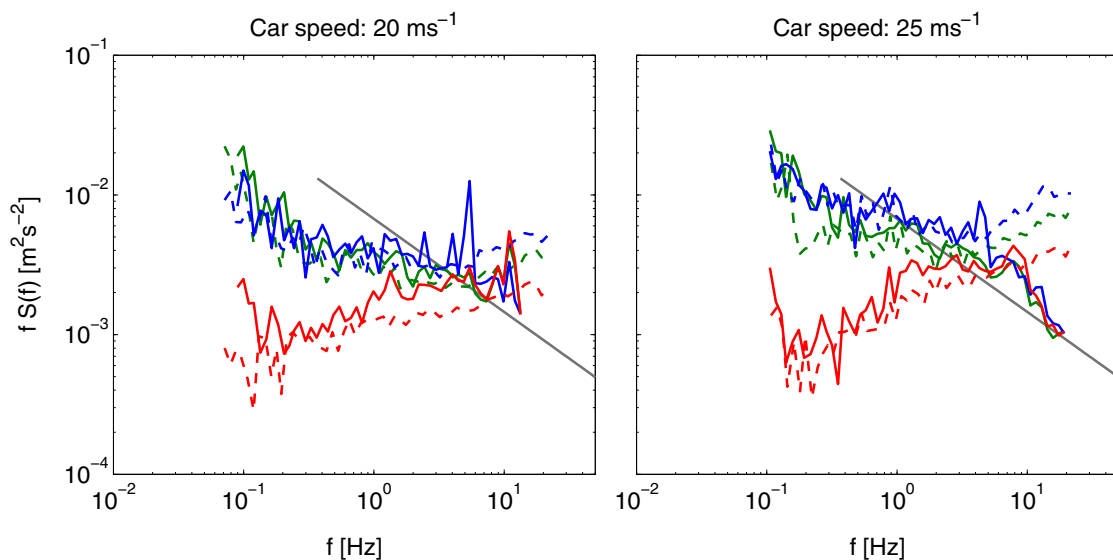


Fig. 7: Corrected power spectra of the longitudinal (green), lateral (blue) and vertical (red) velocity components from the SUMO 5-hole probe ADS (solid line) and the DCF system (dashed line), with frequency ( $f$ ) on the x-axis and spectral energy ( $fS(f)$ ) on the y-axis. The spectra are averaged for consecutive legs with car speeds of approximately 20 and 25  $\text{m s}^{-1}$  to reduce the variability between the individual spectra induced by the low-frequency oscillations of the mounting frame. The theoretically expected  $-2/3$  slope of the inertial subrange is shown by the grey line.

222 component as shown in the experiments by [30–32]. Nevertheless, the 5-hole probe ADS vertical velocity spectra for  
223 the car speed of  $25 \text{ m s}^{-1}$  follows the expected subrange slope. We speculate that this is a consequence of the higher  
224 velocity of the approaching airflow. For the car speed of  $20 \text{ m s}^{-1}$ , the car is still slow enough for the streamlines to  
225 be deflected both horizontally and vertically. When driving with  $25 \text{ m s}^{-1}$ , the streamlines are not able to be sufficient  
226 vertically deviated in front of the car, thus reducing the amount of vertical flow distortion.

227 Despite the flow distortion at the high-frequency end and the peaks introduced by vibrations of the SUMO dummy,  
228 Fig. 7 shows that the spectral components of both systems are in close agreement for both velocity ranges. This  
229 indicates that the 5-hole probe ADS is suitable for turbulence measurements from the RPAS SUMO platform.

## 230 5. Summary and outlook

231 The 5-hole probe ADS turbulence measurement sensor from Aeroprobe has been implemented and tested for the  
232 RPAS SUMO.

233 The 5-hole probe ADS was first tested in a wind tunnel. A parallel experiment together with a hot-wire anemometer  
234 (HW) shows the capability of the probe to react to turbulence in the same manner as the HW system. The resulting  
235 spectra from the two platforms show in general good agreement in the relevant frequency range ( $> 0.02 \text{ Hz}$ ), for both  
236 the laminar and the turbulent case.

237 Thereafter, the effect of varying tubing length between the probe and the air data computer was tested to investigate  
238 potential effects of spectral damping induced by the tubing. For the shortest tubing length of  $15 \text{ cm}$ , already being  
239 used when operating the ADS in SUMO, the system is proven to resolve turbulence satisfactory up to frequencies  
240 around  $20 - 30 \text{ Hz}$ . The spectral damping increases for increasing tubing length.

241 Parallel to two sonic anemometers, the 5-hole probe ADS was mounted on a SUMO airframe at the roof-top of  
242 the institute car to investigate its behavior under real atmospheric conditions. The car was driven for 12 consecutive  
243 straight legs down the runway of Flesland airport, Bergen, Norway, with car speeds of  $20$  and  $25 \text{ m s}^{-1}$ . The com-  
244 ponents of the velocity spectra show that the DCF system suffers from flow distortion, possibly introduced from the  
245 straps used to fix the ladders used as mounting frame and from corner deflection effects of the mounting frame. Do  
246 to technical limitations, the SUMO accelerometers and angular rate sensors were only running with low resolution  
247 during this experiment. Therefore, the peaks associated with vibrations of the SUMO dummy seen in the 5-hole probe  
248 spectra could not be removed. Nevertheless, the velocity spectral components of both the DCF system and the 5-hole  
249 probe ADS are in close resemblance to each other. This indicates that the 5-hole probe ADS is suitable for turbulence  
250 measurements from the RPAS SUMO platform. The environmental test in this study also shows that care must be  
251 taken to avoid flow distortion when constructing a “low-cost, self-made,” instrument mounting frame on the roof-top  
252 of a car. To improve the quality of the turbulence measurements performed in this study, the authors plan a new test  
253 at Flesland airport with an improved mounting design causing less flow distortion, e.g. similar to that one presented  
254 by [33].

## 255 Acknowledgements

256 This work has been funded by a joint research project between Statoil AS and the Geophysical Institute at the  
257 University of Bergen as part of the Norwegian Center for Offshore wind Energy (NORCOWE). The authors are  
258 grateful to Prof. Stephan Lämmlein from the University of Applied Sciences in Regensburg for giving access to the  
259 wind tunnel and to his student Sebastian Wein for performing the wind tunnel tests of the 5-hole probe. Great thanks  
260 are also going to Bjørn Nygaard and his colleagues from the Avinor team at Bergen airport Flesland for making it  
261 possible to use the runway for the environmental comparison of the SUMO system against the sonic anemometers.  
262 Their help and assistance in the preparation and realization of those tests is highly appreciated.

## 263 References

- 264 [1] Sanderse, B., van der Pijl, S.P., Koren, B.. Review of computational fluid dynamics for wind turbine wake aerodynamics. *Wind Energy*  
265 2011;14:799–819.

- 266 [2] Smalikhov, I.N., Banakh, V.A., Pichugina, Y.L., Brewer, W.A., Banta, R.M., Lundquist, J.K., et al. Lidar investigation of atmosphere effect  
267 on a wind turbine wake. *Journal of Atmospheric and Oceanic Technology* 2013;30:25542570.
- 268 [3] Aitken, M.L., Banta, R.M., L., P.Y., Lundquist, J.K.. Quantifying wind turbine wake characteristics from scanning remote sensor data.  
269 *Journal of Atmospheric and Oceanic Technology* 2014;31:765–787.
- 270 [4] Emeis, S. *Surface-Based Remote Sensing of the Atmospheric Boundary Layer*. Springer; 2010.
- 271 [5] Gottschall, J., Courtney, M.S., Wagner, R., Jrgensen, H.E., Antoniou, I. Lidar profilers in the context of wind energya verification procedure  
272 for traceable measurements. *Wind Energy* 2012;15:147–159.
- 273 [6] Bingöl, F., Mann, J., Larsen, G.C.. Light detection and ranging measurements of wake dynamics Part I: One-dimensional Scanning. *Wind*  
274 *Energy* 2010;13:51–61.
- 275 [7] Trujillo, J.J., Bingöl, F., Larsen, G., Mann, J., Kühn, M.. Light detection and ranging measurements of wake dynamics. Part II: two-  
276 dimensional scanning. *Wind Energy* 2011;14:61–75.
- 277 [8] Barthelmie, R.J., Folkerts, L., Larsen, G.C., Rados, K., Pryor, S.C., Frandsen, S.T., et al. Comparison of Wake Model Simulations with  
278 Offshore Wind Turbine Wake Profiles Measured by Sodar. *Journal of Atmospheric and Oceanic Technology* 2006;23:888–901.
- 279 [9] Wharton, S., Lundquist, J.K.. Assessing atmospheric stability and its impacts on rotor-disk wind characteristics at an onshore wind farm.  
280 *Wind Energy* 2011;15:525–546.
- 281 [10] Trombe, P.J., Pinson, P., Vincent, C., Bvith, T., Cutululis, N.A., Draxl, C., et al. Weather radars the new eyes for offshore wind farms?  
282 *Wind Energy* 2013;online first:DOI: 10.1002/we.1659.
- 283 [11] Taylor, G.I.. *The Spectrum of Turbulence*. *Proceedings of the Royal Society of London Series A, Mathematical and Physical Sciences*  
284 1938;164(919):476–490.
- 285 [12] Stull, R.B.. *An Introduction to Boundary Layer Meteorology*. Kluwer Academic Publishing; 1988.
- 286 [13] Reuder, J., Jonassen, M.O.. First Results of Turbulence Measurements in a Wind Park with the Small Unmanned Meteorological Observer  
287 SUMO. *Energy Procedia* 2012;24(0):176–185.
- 288 [14] Kocer, G., Müller, M., Mansour, M., Chokani, N., Abhari, R.S.. Full-Scale Wind Turbine Near-Wake Measurements Using an Instrumented  
289 Uninhabited Aerial Vehicle. *Journal of Solar Energy Engineering* 2011;133(4):doi:10.1115/1.4004707.
- 290 [15] Reuder, J., Brisset, P., Jonassen, M.O., Müller, M., Mayer, S.. The Small Unmanned Meteorological Observer SUMO: A New Tool for  
291 Atmospheric Boundary Layer Research. *Meteorologische Zeitschrift* 2009;18(2):141–147.
- 292 [16] Reuder, J., Jonassen, M.O., Ólafsson, H.. The Small Unmanned Meteorological Observer SUMO: Recent Developments and Applications  
293 of a Micro-UAS for Atmospheric Boundary Layer Research. *Acta Geophysica* 2012;60(5):1454–1473.
- 294 [17] Lenschow, D.H.. *Probing the Atmospheric Boundary Layer: Aircraft Measurements in the Boundary Layer*. American Meteorological  
295 Society; 1986.
- 296 [18] Lenschow, D.H., Spysers-Duran, P. *Measurement Techniques: Air Motion Sensing*. National Center for Atmospheric Research (NCAR)  
297 Research Aviation Facility (RAF) bulletin No 23 1989;:http://www.eol.ucar.edu/raf/Bulletins/bulletin23.html.
- 298 [19] Williams, A., Marcotte, D.. Wind Measurements on a Maneuvering Twin-Engine Turboprop Aircraft Accounting for Flow Distortion. *Journal*  
299 *of Atmospheric and Oceanic Technology* 2000;17(6):795–810. Williams, A Marcotte, D.
- 300 [20] Båserud, L.. *Investigating the Potential of Turbulence Measurements with the RPAS SUMO*. Master; 2013.
- 301 [21] Brisset, P., Drouin, A., Gorraz, M., Huard, P.S.. *The Paparazzi Solution*. Tech. Rep.; 2006.
- 302 [22] Aeroprobe Corporation. *Air Data System Product Manual*. 2013.
- 303 [23] Saint-Gobain Performance Plastics Corporation. *TYGON R-3603 Laboratory and Vacuum Tubing*. 2003.
- 304 [24] Flügge, M., Reuder, J.. Preliminary Results of the NORCOWE Direct Covariance Flux System for Ship based Measurements. *Energy*  
305 *Procedia* 2013;35(0):128–136.
- 306 [25] Gordon, M., Staebler, R.M., Liggio, J., Makar, P., Li, S.M., Wentzell, J., et al. Measurements of Enhanced Turbulent Mixing near  
307 Highways. *Journal of Applied Meteorology and Climatology* 2012;51(9):1618–1632.
- 308 [26] Wilczak, J.M., Oncley, S.P., Stage, S.A.. Sonic anemometer tilt correction algorithms. *Boundary-Layer Meteorology* 2001;99(1):127–150.
- 309 [27] Goldstein, H.. *Classical Mechanics*. Addison-Wesley; 1965.
- 310 [28] Edson, J.B., Hinton, A.A., Prada, K.E., Hare, J.E., Fairall, C.W.. Direct covariance flux estimates from mobile platforms at sea. *Journal of*  
311 *Atmospheric and Oceanic Technology* 1998;15(2):547–562.
- 312 [29] Miller, S.D., Hristov, T.S., Edson, J.B., Frieche, C.A.. Platform motion effects on measurements of turbulence and air-sea exchange over the  
313 open ocean. *Journal of Atmospheric and Oceanic Technology* 2008;25(9):1683–1694.
- 314 [30] Wyngaard, J.C.. The effects of probe-induced flow distortion on atmospheric-turbulence measurements. *Journal of Applied Meteorology*  
315 1981;20(7).
- 316 [31] Oost, W.A., Fairall, C.W., Edson, J.B., Smith, S.D., Anderson, R.J., Wills, J.A.B., et al. Flow distortion calculations and their application  
317 in HEXMAX. *Journal of Atmospheric and Oceanic Technology* 1994;11(2):366–386.
- 318 [32] Miller, D.O., Tong, C.N., Wyngaard, J.C.. The effects of probe-induced flow distortion on velocity covariances: Field observations.  
319 *Boundary-Layer Meteorology* 1999;91(3):483–493.
- 320 [33] Belušić, D., Lenschow, D.H., Tapper, N.J.. Performance of a mobile car platform for mean wind and turbulence measurements. *Atmospheric*  
321 *Measurement Techniques Discuss* 2014;7(1):949–978.